#3

PROBE STUDIES OF ENERGY DISTRIBUTIONS AND RADIAL POTENTIAL VARIATIONS IN A LOW-PRESSURE MERCURY ARC

R. M. HOWE

TECHNICAL REPORT NO. 221

JANUARY 18, 1952

RESEARCH LABORATORY OF ELECTRONICS
MASSACHUSETTS INSTITUTE OF TECHNOLOGY
CAMBRIDGE, MASSACHUSETTS

The research reported in this document was made possible through support extended the Massachusetts Institute of Technology, Research Laboratory of Electronics, jointly by the Army Signal Corps, the Navy Department (Office of Naval Research) and the Air Force (Air Materiel Command), under Signal Corps Contract No. DA36-039 sc-100, Project No. 8-102B-0; Department of the Army Project No. 3-99-10-022.

MASSACHUSETTS INSTITUTE OF TECHNOLOGY

RESEARCH LABORATORY OF ELECTRONICS

Technical Report No. 221 January 18, 1952

PROBE STUDIES OF ENERGY DISTRIBUTIONS AND RADIAL POTENTIAL VARIATIONS IN A LOW-PRESSURE MERCURY ARC

R. M. Howe

This report is based on a doctoral thesis in the Department of Physics, Massachusetts Institute of Technology, 1950.

Abstract

Probe measurements were made in the plasma of a low-pressure mercury arc. The electron-energy distributions showed depletions from a Maxwellian distribution in the high-energy range. Coupling effects between adjacent probes were investigated and were found to be quite small but in the proper direction to agree with the Langmuir-Tonks theory. Drift-current distortion of the random electron-energy distributions was measured with a bidirectional probe and compared with theory. A multisection probe extending from tube axis to tube wall allowed a determination of radial potential and density variations. Results over a pressure range from 3.4 microns to 3.5 microns showed good agreement with the ambipolar diffusion theory based on cumulative ionization. A direct calculation of ionization rate in the plasma was made from the ionization probability for a one-step ionizing process; comparison of this calculation with the observed ionization rate at 1.7 microns indicated that at that pressure the ionization is half direct, half cumulative. For higher arc pressures cumulative ionization evidently predominates.

PROBE STUDIES OF ENERGY DISTRIBUTIONS AND RADIAL POTENTIAL VARIATIONS IN A LOW-PRESSURE MERCURY ARC

I. Introduction

The study of the positive column of a low-pressure mercury arc by means of probes has been the subject of many researches in the past twenty-five years. The wide interest in this field undoubtedly stemmed from the initial work in 1924 of Langmuir and Mott-Smith (1), who pointed out the incorrectness of the previous practice of obtaining plasma potentials by finding the voltage at which a probe inserted in the plasma drew no net current. They showed that a complete voltage-current characteristic for the probe must be considered, from which one can obtain the true plasma potential as well as much additional information concerning the physical processes taking place in the plasma of the arc.

The original Langmuir-probe type of analysis, successful as it was, left several things unexplained. The Langmuir-Tonks (2) theory of 1929 was a logical attempt to account for at least one of these difficulties but it, too, seemed to present additional discrepancies with experiment.

The purpose of the research described here was to restudy the positive column (plasma) of the low-pressure mercury arc by employing both improved vacuum and measuring techniques now available. In particular, an attempt was made to study the electron-energy distributions in the plasma with considerable exactness by means of probes, and to obtain improvements over Killian's original determinations (3) of radial variations of plasma potential and density in a cylindrical discharge.

II. Probe Theory

The positive column of a mercury-arc discharge consists of a luminous plasma having very nearly equal densities of positive ions and electrons. The electrons are known to possess something approximating a Maxwellian distribution of energies, whereas the energy distribution of the positive ions is not known. If a plane probe is inserted in the positive column, the electric current to the probe will be a function of probe voltage. When the probe is very negative with respect to the plasma, only positive ions will be collected; when the probe is positive with respect to the plasma, electrons directed at the probe will be collected. When the probe is somewhat negative with respect to the plasma, only those electrons which are energetic enough to overcome the retarding potential will be collected along with the positive ions. By subtracting the positive ion current from the total probe current, we obtain the electron current i_-. A plot of log i_- vs V, the probe potential with respect to the anode, is commonly known as the probe characteristic curve (for example, see Fig. 8).

For a Maxwellian distribution of electrons the electron current to a collector of area A is given by

$$i_- = An_- e \left(\frac{kT_-}{2\pi m}\right)^{1/2} \exp\left(\frac{-e(V_p - V)}{kT_-}\right) \quad \text{for } V \leq V_p \tag{1}$$

where n_-, e, m, and T_- are electron density, charge, mass, and temperature, respectively; k is Boltzmann's constant; and V_p is the plasma potential with respect to the anode. A plot of log i_- vs V will yield a straight line having a slope $0.434e/kT_-$ from which the electron temperature T_- can be calculated. Probe curves from low-pressure mercury arcs are nearly always roughly linear and hence represent approximate Maxwellian distributions. Knowing T_- and the total random electron current I_- (as measured for the probe slightly positive with respect to the plasma) we can calculate the electron density n_-.

This probe theory assumes that the presence of the probe in the plasma does not disturb the plasma potential. Langmuir originally assumed (1) that this is possible because a space-charge sheath of small thickness forms around the probe when the potential of the probe is different from that of the plasma. For negative probe voltages this sheath consists of positive ions; for positive probe voltages the sheath consists of electrons. In either case, the voltage drop between probe and plasma takes place over the relatively narrow region of the sheath. By applying the Langmuir-Childs equation for space-charge-limited current, one can show that for plane probes of reasonable size (a few millimeters across) the sheath thickness is small compared with the probe diameter. For a cylindrical probe whose diameter is small compared with sheath thickness it can be shown (4) from the space-charge equation that the positive-ion current is proportional to $(V_p - V)^{1/2}$. This relationship is observed experimentally for a thin wire collector (5).

If the sheath picture is correct, we should be able to make an estimate of the expected ratio of the saturated electron current I_- to the saturated positive-ion current I_+, based on the assumption that the positive ions as well as the electrons have a Maxwellian distribution. For the electric-field gradients observed in the plasma it is easy to show that the electron density n_- is many orders of magnitude greater than the net charge density $n_+ - n_-$ (where n_+ is the positive-ion density). Therefore $n_+ \approx n_-$, and from Eq. 1 and its equivalent expression for positive ions we can solve for I_-/I_+ by setting $V_p = V$. Thus

$$\frac{I_-}{I_+} = \left(\frac{T_-}{T_+}\right)^{1/2} \left(\frac{M}{m}\right)^{1/2} \tag{1a}$$

where T_+ is the positive-ion temperature, and M is the mass of the positive ions. It is reasonable that the positive ions will have a temperature associated with random motion which is not greater than the electron temperature T_- and more likely much less than T_-. Hence $T_-/T_+ \geq 1$, and from Eq. 1a, $I_-/I_+ \geq 605$ for mercury. But actual probe measurements of I_-/I_+ invariably yield ratios between 200 and 400. On the basis of a Maxwellian distribution in positive-ion energies, therefore, it would appear that we

are collecting far too much positive-ion current.

Several possible explanations for this perplexity are apparent when one realizes that the arrival of a positive ion at the probe surface cannot be distinguished from the departure of an electron. Electrons might be leaving for the following reasons:

1. The arrival of positive ions can cause electrons to be ejected (6), probably due to the energy released upon recombination at the surface.
2. The absorption of ultraviolet light at the probe surface will eject photoelectrons (7).
3. Metastable mercury atoms may cause the emission of electrons when they strike the probe surface and lose their energy of excitation (8).

If the negative-voltage saturation current to the probe does not consist entirely of the arrival of positive ions, the energy delivered to the probe should be less than that calculated on the basis of positive-ion current alone. Several attempts to verify this have been made utilizing electrically heated probes. Oliphant (9) finds evidence of electron emission from probes in rare-gas discharges, while Molthan (10) concludes that there is no appreciable electron emission.

It appears doubtful if any of the above effects are capable of explaining the very considerable lack of agreement between the random-current theory and the experimentally observed positive-ion currents to the probe. Rather, the answer to the dilemma would seem to lie in the original assumption that the presence of the negative probe has not altered the plasma potential immediately outside the sheath. Under this assumption positive ions which strike the sheath are accelerated toward the probe and collected. Thus at the boundary of the sheath all positive ions are moving toward the probe surface. But to say that the plasma potential just beyond this boundary is unchanged despite the presence of the adjacent sheath is to claim that the positive ions have random motions in all directions. This transition from completely random motions to directed motions obviously cannot take place in an infinitely short distance, but requires a distance of the order of mean free paths of the positive ions. As we move from the region of complete random motion, through the transition region, to the edge of the sheath, the plasma potential will be slowly decreasing. The result is a shallow potential well for positive ions extending many sheath thicknesses beyond the sheath itself. It is possible for this shallow potential well to account for the observed positive-ion current, which is too large to be due to purely random current collected by the surface of the space-charge sheath. This idea is treated quantitatively in the Langmuir-Tonks theory (2) and will be discussed in the light of some experimental results later in this article.

III. Apparatus

A. Description of the Mercury-Arc Tube

Although probe measurements were made in three different tubes, most of the data were obtained from the tube shown in Fig. 1. The envelope of this tube is made of pyrex glass and is circular in cross section, so that the geometry of the main body is

cylindrical. A pool of mercury at the bottom of the vertical section serves as the cathode. There are two anodes: a cylindrical main anode and a disk-shaped auxiliary anode (for the purpose of stabilizing the arc). All press leads are tungsten, while the anode and probe structures are made of tantalum.

The three probe assemblies used in the tube of Fig. 1 are shown in greater detail in Fig. 2. The swivel probe consists of a plane disk-shaped collector which is hinged so that its axis can be swung either parallel or perpendicular to the axis of the tube.

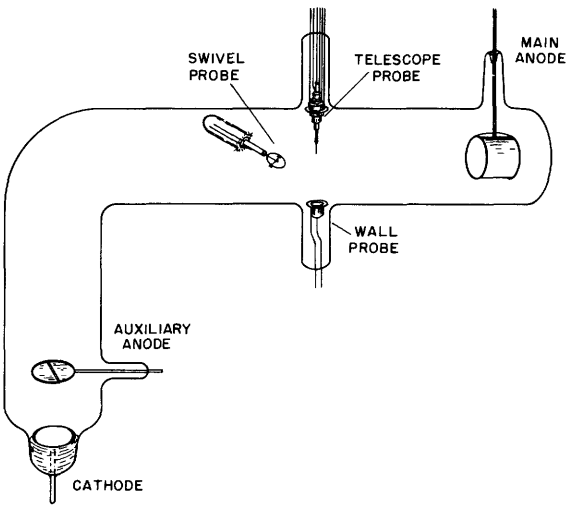

Fig. 1
Mercury-arc tube.

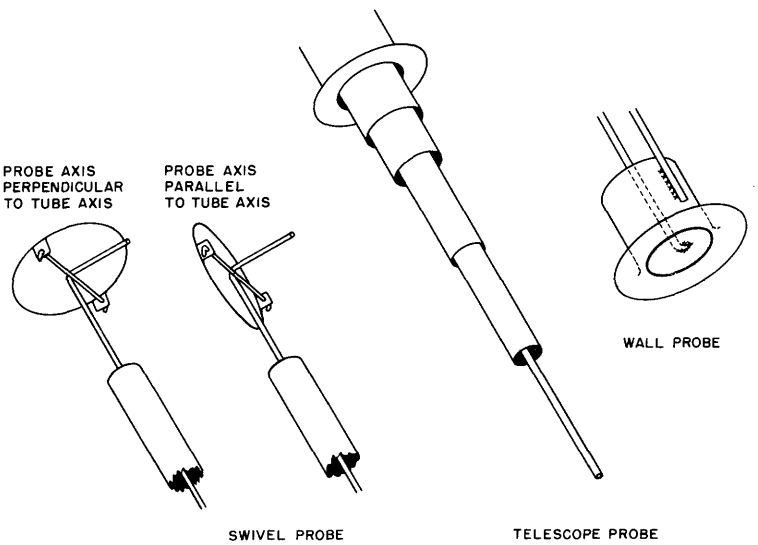

Fig. 2
Probe assemblies.

This probe is used to study the effect of drift current on the probe characteristics. The supporting stem of the swivel probe is shielded from the plasma by a cylindrical guard extending from probe to wall. The telescope probe is an array consisting of five coaxial cylinders extending from tube axis to tube wall. The exposed portion of each cylinder serves as a collector as well as a shield for the cylinders inside. This probe assembly is used to study radial variation in plasma properties. Diametrically opposite the telescope probe is the wall probe, which is a plane disk-shaped collector mounted flush with the tube wall and surrounded by a shield.

All probe and shield surfaces are constructed of 3-mil tantalum sheet. Probes and shields are insulated from each other simply by mechanical clearance resulting from careful alignment.

The above description applies to the tube shown in Fig. 1. Two other tubes were used. The first was almost identical in geometry with the tube described except for a shorter vertical section in its envelope; the second tube had a straight envelope with no bend and was mounted vertically. Only plane probes were used in these latter two tubes, and results were similar to those obtained with the tube in Fig. 1.

B. Processing of the Tube

Before the probes and shields were mounted on the press leads, the tube was baked for a number of hours at 500°C while under high vacuum. Main and auxiliary anodes were outgassed by heating to about 1500°C with rf induction. This procedure allowed a preliminary check for leaks in the many presses. The side tubes supporting the presses were then cracked off about 3/4 inch from the press ends to permit easy access with the spot welder to the tungsten leads.

All probe assembly components were pre-outgassed at a temperature of about 1900°C by mounting them in dummy tubes and bombarding them with 2000-volt electrons. The parts were then welded to the press leads, which finally were sealed back onto the main envelope. The completed tube was sealed onto the vacuum system along with two mercury stills. The inner still and the mercury-arc tube were baked at 500°C under high vacuum, after which clean mercury in the outer still was distilled into the inner still. The outer still was then sealed off of the system, and mercury from the inner still was distilled into the tube proper. After the electrodes had been outgassed by rf induction, the arc was lit by touching a high-voltage spark generator to the outside of the mercury bulb. Tube current was increased until both anodes were red, and this condition was maintained for several hours. During the latter portion of this run the vacuum, as measured by the centimeters stick of a McLeod gauge, was as good as that observed when the arc was off. In addition, all probes were flashed white-hot by driving them to anode potential or higher. For wall probes it was necessary to cause the arc to transfer partially to the probe in order to get adequate heating.

After replenishing the supply of mercury in the bulb of the discharge tube, the inner still was sealed off of the system and the pumping lead to the tube itself preheated.

Again the tube was run under extreme overload for about 30 minutes, after which the final seal-off was made. All probe measurements were made with the tube sealed off of the vacuum system.

C. Bath Arrangement

Early experimenters with mercury arcs controlled the pressure of the discharge by varying the temperature of a water bath surrounding the mercury-bulb portion of the tube. Care was usually taken to maintain other sections of the tube at temperatures above the bath temperature in order to discourage the condensation of mercury on these other sections. The pressure of the mercury gas in the tube was then taken as the vapor pressure of mercury at bath temperature.

Klarfeld (11) has pointed out that this procedure is apt to lead to considerable error in the calculation of mercury pressure, and that the best procedure is to submerge the entire tube in a water bath of constant temperature. With this arrangement mercury droplets condense over all portions of the tube; since all these regions are at the same temperature, a constant pressure equal to the vapor pressure of mercury at water-bath (and hence tube-wall) temperature is assured.

This technique has been used in the research described here. The entire tube was submerged in a tank filled with water. Good circulation of the water was provided by a stirring paddle turned by a small induction motor. The resulting turbulence maintained the bath temperature constant to within 0.1°C throughout the tank. There is a small correction (of the order of 1°C) between bath temperature and inner-wall temperature of the tube due to the conduction of heat out through the tube walls.

The first probe measurements were taken with only the bulb of the mercury tube cooled by water. Later, when the tube was entirely immersed, the pressure decreased by a factor of about twenty, which is graphic proof of the importance of completely submerging a mercury-arc tube in water if accurate knowledge of the pressure is desired.

IV. Measurement Techniques

A. Contact Potential Shifts

It was observed that the contact potential of the probe surface changes with time after the probe is flashed red-hot by electron bombardment. This shift in contact potential is found by observing the probe current as a function of time after flash for a probe voltage close to the floating potential. In this region of probe voltage the positive-ion and electron currents nearly balance, and as a result the net probe current is very sensitive to a small change in contact potential (since electron current varies exponentially with probe voltage). A typical plot of contact-potential shift vs time after flash is shown in Fig. 3. It is apparent from the curve that some 10 sec elapse before the contact potential begins to change.

The following observations indicate that this change in contact potential of the probe

surface is an effect due to mercury settling on the probe surface and not due to contaminating gas.

1. The change in contact potential is of the same magnitude and has the same time constant for all three of the experimental tubes used, even when the tubes are being pumped on the vacuum system.
2. Probe assemblies which allow faster conduction of heat away from the probe surface exhibit a shorter time constant and a slightly greater contact-potential shift. This is consistent with the hypothesis that the change in contact potential is a temperature effect; the cooler the probe, the more mercury can be present in equilibrium on the surface.
3. For a given arc current the change in contact potential is greater for lower mercury pressures. Again this is in agreement with the temperature hypothesis, since at lower pressures the random currents are lower. This means that heating effects due to positive ion and electron bombardment at the floating potential will be less. Thus the final equilibrium probe temperature will be lower.
4. The change in contact potential observed corresponds to a lowering of the work function, which is what is expected for a surface layer of electropositive atoms such as mercury. On the other hand, oxygen and nitrogen are known to raise the work function of a surface when they adsorb on it.

This shift in contact potential makes it imperative to flash the probe red-hot before each current reading. Otherwise, a gradual shift in probe-contact potential takes place as the probe voltage is varied from very negative values up to plasma potential. To get sufficient heating for probes located near or at the tube wall it is necessary to run the probe to a voltage high enough to cause the arc to transfer to the probe. A resistor in series with the probe serves to limit the current to the desired value after the arc has transferred.

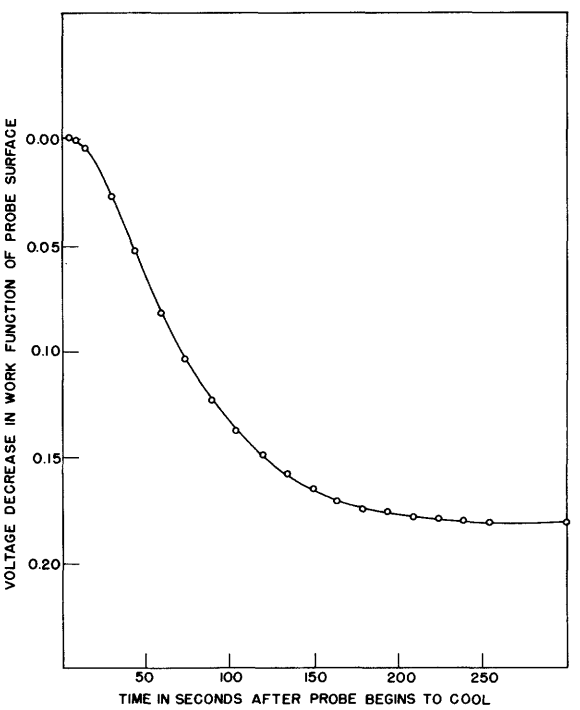

Fig. 3
Contact-potential shift.

It is interesting to note that no change in positive-saturation current for very negative probe voltages was observed after a flash. This would indicate that no important photoelectric or metastable effects are taking place at the probe surface, since such effects would probably be quite dependent on the surface state of the probe.

B. Extrapolation of Positive-Ion Current

A determination of the positive-ion current is extremely important in a study of electron-energy distributions from probe curves, since it is the positive-ion current which must be subtracted from

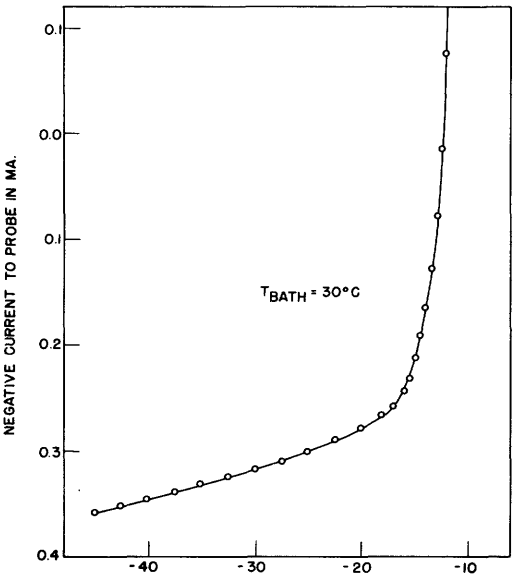

Fig. 4
Voltage-current curve for wire probe.

the total probe current in order to obtain the electron current. This need for an accurate knowledge of the positive-ion current i_+ is particularly important in the voltage range where i_+ and the total probe current i_p are nearly equal, and where the electron current i_- is therefore a small difference.

The only method of obtaining i_+ for various probe voltages is to use an extrapolation from the negative-voltage saturation region of the probe curve, since in this region we believe we are collecting no electrons. For a plane collector, the positive-ion saturation curve is usually fairly linear, particularly at higher mercury pressures; but for small cylindrical collectors, the plot may have considerable curvature, as can be seen in Fig. 4. Where a definite curvature exists, one empirical approach makes use of a plot of log i_p vs log $(V_p - V)$, where $(V_p - V)$ is the retarding potential of the probe relative to plasma potential. When this method is used (as in Fig. 5) one obtains a fairly linear saturation curve. The departure from linearity due to the start of electron collection is much more clearly marked, and the value of i_+ is taken from the linear extrapolation on this log-log plot.

All this method attempts to do is maintain an i_p vs V trend established in the negative-voltage region of saturation, so that one can make reasonable guesses for i_+ and hence i_-. Obviously one cannot take too seriously values of i_- which are very much less than i_p (i.e. obtained from the small difference between i_+ and i_p). It is also apparent that for values of i_- of the same order as or greater than i_p, any subtle differences in i_+ extrapolation techniques cannot affect appreciably the value of i_-.

C. Oscillations

A DuMont 224A Oscilloscope was used to monitor cathode-to-anode potential and probe-to-anode potential. Oscillations up to 5 Mc/sec could have been detected, but nothing other than random noise or "grass" was ever observed on the oscilloscope. Later attempts to detect oscillations at frequencies up to 1000 Mc/sec yielded negative results.

D. Tube Current

All probe measurements were taken with a cathode-to-main-anode current of 4 amp and a cathode-to-keeping-anode current of 2 amp. Increasing the currents much above

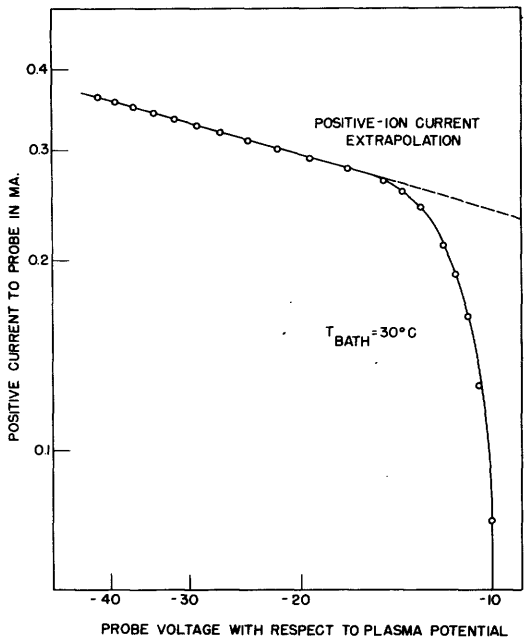

Fig. 5
Log voltage—log current curve for wire probe.

these figures resulted in overheating of the anodes, while decreasing the main-anode current below approximately 2 amp usually caused the arc to go out within a few minutes. An additional keeping-anode located at the top of the vertical section of the tube would probably have stabilized the arc sufficiently to permit the use of much lower currents to the main anode.

E. Inconsistent Results for Bath Temperatures in the 50°C Region

At bath temperatures in the 50°C region the probe curves seemed to be nonreproducible at times, particularly for probe voltages a little below plasma potential. The reason for these fluctuations was never determined. No changes in arc voltage were observed either with the dc meter or the oscilloscope. Perhaps this pressure range lies in a transition region between two stable conditions of the arc.

F. Current-Density Discrepancy between Wire Probe and Swivel Probe

Both the swivel probe and wire probe are located at the tube axis. Hence the ratio of electron currents collected by the two probes should be the same as the ratio of their areas, i.e. 0.60 cm^2/0.13 cm^2 = 4.6. The observed ratio of electron currents is 3.2 for 22°C, 30°C, and 40°C baths. The discrepancy may lie in the uncertainty in determining the area of the swivel probe. This probe is a complicated structure, and it is difficult to estimate what fraction of the area is effective in collecting electrons. The 0.60 cm^2 area used above represents the total of all the area, including both front and back sides of the disk and tabs as well as the exposed portion of the supporting stem

(see Fig. 2). The effective swivel-probe area for collecting electrons may be considerably less than this total area.

V. Coupling Effects between Probes

Simple probe theory assumes that the presence of the probe in the plasma does not appreciably alter the plasma potential. The validity of this assumption can be tested experimentally by observing whether the potential of one probe affects the current collected at an adjacent probe. For example, the characteristic curve of the wire probe can be observed for different potentials of the first surrounding shield. Several important facts are apparent from these measurements.

First of all, as the shield voltage is varied from -12 to +1 volt with respect to the plasma, the wire-probe curves shift to the right by approximately 0.2 volt. This indicates that the presence of the shield at a potential negative with respect to the plasma has shifted the plasma potential itself to a slightly more negative value. This lowering of the plasma potential as a result of the presence of a surface at negative potential in the plasma is consistent with the Langmuir-Tonks theory discussed earlier, in which it is argued that, due to the flow of positive ions into the wall (or probe) surface where recombination takes place, a rather shallow potential well for the positive ions is set up around this surface. In our case the 0.2-volt shift is rather smaller than one might expect, but we are, of course, dealing here with a much smaller surface than the tube wall. We must also remember that the 0.2-volt shift is only the average effect the shield exerts on the entire plasma surrounding the wire probe. The shift in plasma potential may, in fact, be much larger right next to the shield.

Secondly, we find that as the shield is made positive, the positive-ion current to the wire probe decreases by 2 percent; yet at the same time the total electron current increases by approximately 1.5 percent. Both of these effects are in a direction suggesting that, as the shield potential is changed from negative to positive, the potential of the plasma surrounding the wire probe is raised slightly. In other words, at negative voltages the shield causes a lowering of the plasma potential over a fairly broad region.

In summary of these coupling tests, I feel that they show that by far the greater part of the potential drop between a negative probe and the plasma takes place over a very narrow sheath region. However, there is evidence that there exists an additional small voltage drop extending over a considerable region of the plasma, as postulated by Langmuir and Tonks. Because of the smallness of the coupling effect observed, all probe measurements with the exception of coupling tests themselves were taken with the shields floating.

VI. Evaluation of Drift-Current Effect

By means of the swivel probe it is possible to investigate distortion of the probe-characteristic curve resulting from the effect of drift current. When the probe is

oriented so that its axis is perpendicular to the tube axis, it receives only random current. When the probe is oriented such that its axis is parallel to the tube axis, it is subjected to drift current as well as random current. Note that in the latter position the two sides of the probe are facing the cathode and anode, respectively. This means that any departures from the random-current probe characteristic will be a result only of second-order changes in the distribution function due to effects of the drift current.

Let us assume that when drift current is present, the spherically symmetrical distribution in electron momentum is displaced linearly in momentum space by an amount equal to the drift momentum. Starting with a Maxwellian distribution, we write for our new distribution

$$f(p_x, p_y, p_z) = n_-(2\pi mkT)^{-3/2} \exp\left[-\frac{(p_x - p_o)^2 + p_y^2 + p_z^2}{2mkT}\right] \qquad (2)$$

where $p_{x,y,z}$ = the momentum in x, y, and z directions, respectively, and p_o = the momentum associated with the drift velocity. The current density i_d to a probe at potential V relative to plasma potential V_p is given by

$$i_d(V) = e \int_{p_x=\sqrt{2me(V_p - V)}}^{p_x=\infty} \int_{p_y=-\infty}^{p_y=\infty} \int_{p_z=-\infty}^{p_z=\infty} \frac{p_x}{m} f(p_x, p_y, p_z)\, dp_x dp_y dp_z \qquad (3)$$

where the probe surface is normal to the x direction. After the integration has been performed we have

$$i_d(V) = n_- e(2\pi mkT)^{-3/2} \left\{ \exp\left[-\left(\sqrt{\frac{e(V_p - V)}{kT}} - \frac{a}{2\sqrt{\pi}}\right)^2\right] + \frac{a}{2}\left[1 - \operatorname{erf}\left(\sqrt{\frac{e(V_p - V)}{kT}} - \frac{a}{2\sqrt{\pi}}\right)\right]\right\} \qquad (4)$$

where a is the magnitude of the ratio of drift current to random current. For the side of the probe facing the cathode, the drift current and random current are in the same direction and therefore a is positive; for the side facing the anode, their directions are opposite and a is negative.

It seems reasonable to assume that the drift current at any point across the tube is proportional to the electron density n_- at that point. From the telescope probe measurements we know n_- across the tube; from the total tube current we can then calculate the drift-current density at the tube axis. When this is done at a bath temperature of 22°C and a tube current of 4 amp, a turns out to be 1.05. From Eq. 4 we can find the current to both sides of the plane probe. This calculated current is compared with the

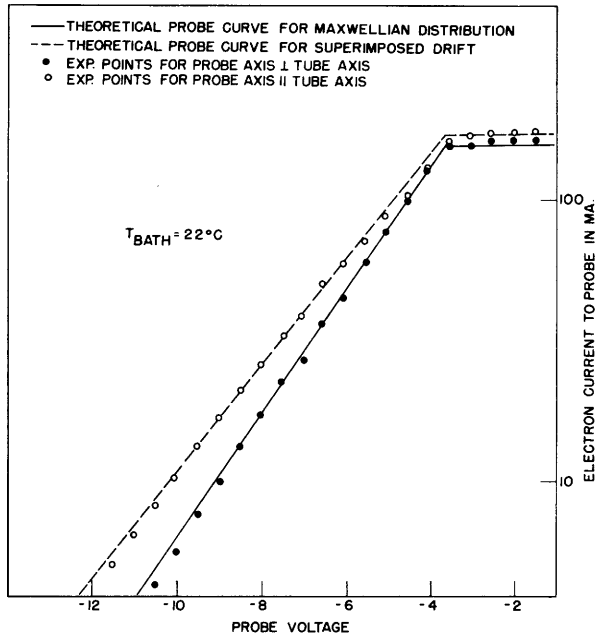

Fig. 6

Comparison of theoretical and experimental drift-current effects.

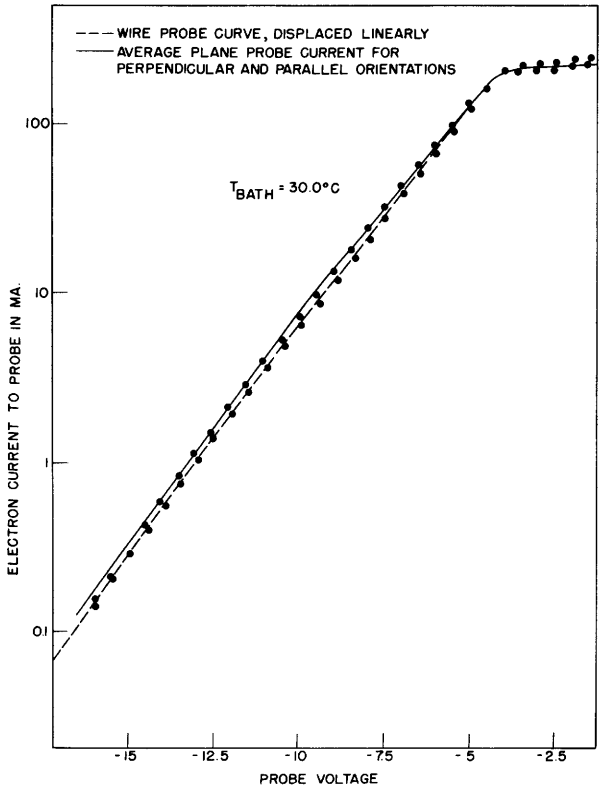

Fig. 7

Comparison of average drift-random effect with wire-probe curve.

observed currents in Fig. 6. The agreement seems good over the range in which the distribution is Maxwellian, indicating that our original assumption that the symmetrical distribution was displaced linearly in velocity space was not unreasonable.

It is apparent from Fig. 6 that there is no appreciable difference between total electron current or plasma potential as measured with the two orientations; nor, it turns out, is there any appreciable difference in positive-ion currents. The greatest distortion of random-current curves by drift current occurs at the lowest pressures; distortion almost disappears for a bath temperature of 61.5°C.

The various members of the telescope array are subject, on the average, to the collection of both pure random current (corresponding to the perpendicular orientation of the swivel probe) and to random plus drift current (corresponding to the parallel orientation of the swivel probe). Hence, the average probe current for the two swivel-probe orientations should yield a probe characteristic curve similar to that obtained for the wire probe, which is the central member of the telescope array. Figure 7 shows that this is true.

As a result of these considerations we can say that the members of the telescope-probe array will give us good plasma potentials and total electron currents, but that the shape of the actual probe curves cannot be taken as an exact measure of the electron-energy distribution except at the highest pressures used. At these highest pressures the wire probe will, in fact, probably give a better indication than the plane probe of true electron-energy distribution because of the much smaller collecting area of the wire probe.

VII. Electron-Energy Distributions in the Plasma

Probe measurements in the plasma of arc discharges nearly always show deviations from Maxwellian distributions in the high-energy electron region. These deviations show up as departures from linearity in the retarding-potential region of the probe characteristic curve. In Figs. 8, 9, and 10 are shown probe curves at the tube axis for bath temperatures of 22°C, 40°C, and 61.5°C. Wall-probe curves are similar. All the curves exhibit a bilinear character in which the upper, straight-line portion of the curves represents from 95 percent to 99 percent of the electron current. The lower region of the curves would seem to indicate a deficiency of electrons from a Maxwellian distribution.

It is not possible to tell conclusively from the probe curve whether a given departure from linearity represents a depletion or a surplus of electrons from a Maxwellian distribution. This was first pointed out by Druyvesteyn (12), who showed that one could obtain the actual electron-energy distribution by a method which involves taking the second derivative d^2i_-/dV^2, where i_- is the electron current to the probe and V is the probe voltage. To do this from the probe curve itself results in considerable inaccuracy, but the second derivative can be obtained directly from probe measurements by

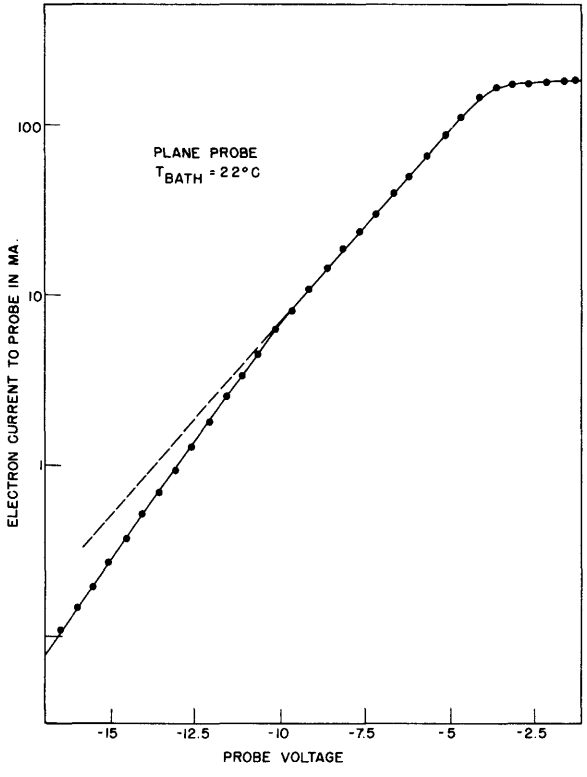

Fig. 8
Characteristic curve of plane probe for 22°C bath.

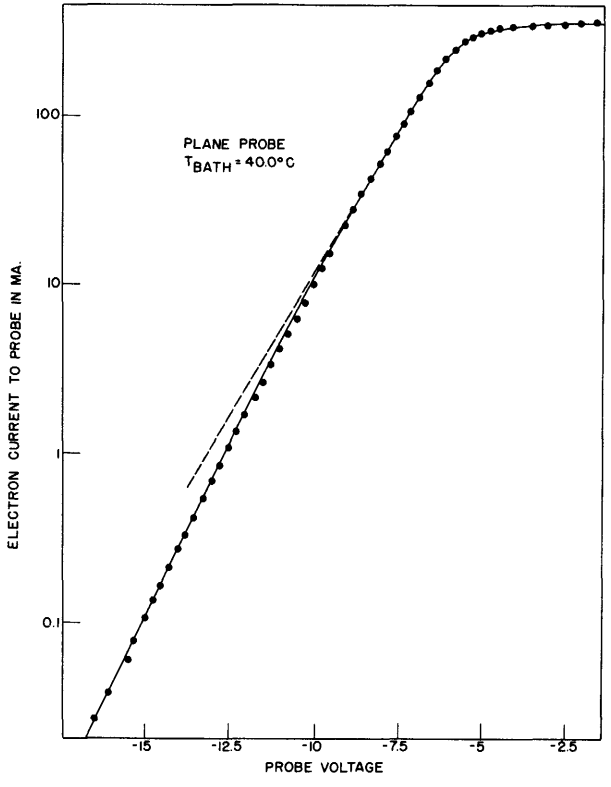

Fig. 9
Characteristic curve of plane probe for 40°C bath.

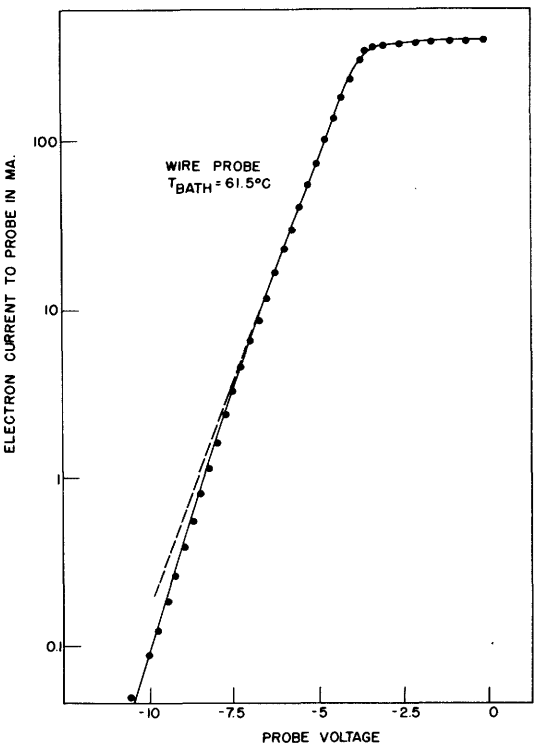

Fig. 10
Characteristic curve of wire probe for 61.5°C bath.

observing the increase in probe current when a small sinusoidal voltage is superimposed on the dc probe voltage (13).

Despite the questionable correlation between probe curves and actual energy distributions, it seems evident that the curves of Figs. 8, 9, and 10 do represent a depletion from a Maxwellian distribution in the high-energy region, since there are several reasons why we should expect such a depletion. First, electrons are continually making collisions with mercury atoms, and there is a probability that these collisions will be inelastic for electrons with energies above approximately 5 volts; such collisions result either in excitation or ionization of the unexcited mercury atoms (14). Also, the concentration of excited atoms, particularly metastables, may be an appreciable fraction of the concentration of all mercury atoms, and inelastic collisions with these excited atoms may produce additional excitation or ionization. We know that ions are being produced in the plasma at a considerable rate. Whether the ionization is the result of a single collision or of multiple collisions with electrons, it is clear that for every ion which is created there must have been at least one inelastic collision by an electron, a collision which results in a very large loss of energy for that electron. Therefore, the very existence of an ionization process demands a net transfer of electrons in velocity-space through the distribution from low energies to high energies, where they suffer inelastic collisions and drop back again to low energies. In order to maintain this

unbalance from thermal equilibrium there must be a depletion in the high-energy range from a Maxwellian distribution.

There is another reason for expecting this depletion. From measurements with the wall probe we can find its floating potential, i.e. the potential for which the net flow of current to the probe is zero. If we assume that the adsorption fractions for mercury ions and electrons are the same for both glass and tantalum, respectively (15), then the floating potential of the probe is equal to the potential of the glass walls of the tube, since these glass walls can receive no net current. Furthermore, if the adsorption fractions are not exactly the same, the wall potential still will not be very different from the floating potential of the probe, since the electron current varies so markedly with small voltage changes.

The potential of the tube walls will thus be fairly negative with respect to the plasma near the walls (-4.5 volts for a 61.5°C bath, -10 volts at 22°C). This voltage drop takes place over the positive-ion sheath at the walls. Most of the low-energy electrons which are directed toward the walls will be reflected back into the plasma. Only those which have an energy associated with motion normal to the walls that is large enough to overcome the retarding potential of the sheath can stick to the glass walls. The current of these high-energy electrons flowing into the walls is just enough to balance the positive-ion current flowing to the wall; recombination then takes place at the wall.

In order to maintain this selective flow of high-energy electrons into the wall the distribution must again exhibit a depletion of high-energy electrons from a Maxwellian distribution. In the plasma region near the walls this depletion should be quite noticeable. As we go a number of mean-free paths away from the wall, the depletion due to wall currents will gradually disappear as the motions again become random. The mean-free path, as calculated from Brode (16), is about equal to the tube radius at 22°C bath temperature, so that depletion due to wall current should be present in the distribution at the tube axis. At 40°C, however, the mean-free path is only about one-sixth of the tube radius, so that depletion effects of the wall should be smoothed out in the distribution at the axis. However, depletions due to exciting or ionizing collisions will be present in the distribution at both the tube wall and axis.

Professor W. P. Allis has calculated the distribution function necessary to cause a net transfer of electrons in velocity-space through the distribution from low energies to high energies. In this derivation he has assumed that the electron-electron interaction cross section varies inversely as the energy squared. The resulting distribution can be represented approximately by

$$f(u)\,du = Au^{1/2}\left[e^{\frac{u_o-u}{\theta}} - 1\right]du \qquad u < u_o$$
$$= 0 \qquad\qquad\qquad\qquad u > u_o \tag{5}$$

where

u = energy of the electron

$\theta = 2/3\ \bar{u}$ ($\bar{u}$ = the average energy)

A = a constant depending on the electron density

u_o = a constant depending on the net rate of flow through velocity-space.

The approximation is good for $u_o/\theta > 5$.

This distribution evidently goes to zero at $u = u_o$. This is because the distribution has been calculated such that there is a constant flow of electrons through velocity-space toward higher energies; at $u = u_o$ the distribution has merely died out in the act of trying to furnish this flow of electrons. In an actual case where such a distribution applies, the inelastic collisions which cause the flow through velocity-space will begin to set in at an energy u_1 which is considerably less than u_o. If the probability for inelastic collisions as a function of energy u is known, then a second theoretical distribution can be calculated for $u > u_1$ and patched onto the $f(u)$ distribution at $u = u_1$.

From the distribution $f(u)$ the following formula for the random current collected on the surface of a plane probe is obtained:

$$I_p(V) = C\left\{ e^{\frac{u_o - eV}{\theta}} - \left[1 + \frac{(u_o - eV)}{2\theta^2} \right] \right\} \qquad 0 < eV < u_o$$

$$= 0 \qquad eV > u_o \tag{6}$$

where

$-V$ = the probe voltage relative to the plasma

C = a constant depending on the electron density.

In Fig. 11 the probe curve calculated from Eq. 6 is compared with the experimental currents for the plane probe at 30°C bath temperature. θ was obtained from the slope of the upper straight-line portion of the experimental probe curve, and the theoretical curve was translated linearly until a good fit with the experimental points was obtained. Note that the agreement between the experiment and theory is good to approximately -14 volts (actually -10 volts with respect to plasma potential). The point of departure from the theory lies in the very region where inelastic collisions with the wall, as well as ionizing collisions, begin, and where the calculated distribution can therefore no longer be correct.

A similar agreement between the calculated distribution and experiment is shown in Fig. 12, where the wire-probe data are compared with theory at a bath temperature of 61.5°C. The plane-probe data at this high pressure do not show such good agreement, but the wire probe is believed to yield more reliable results because of its smaller area and because drift current is negligible at 61.5°C. Good agreement between experimental and theoretical probe curves is also obtained at 40°C and 50°C bath temperatures.

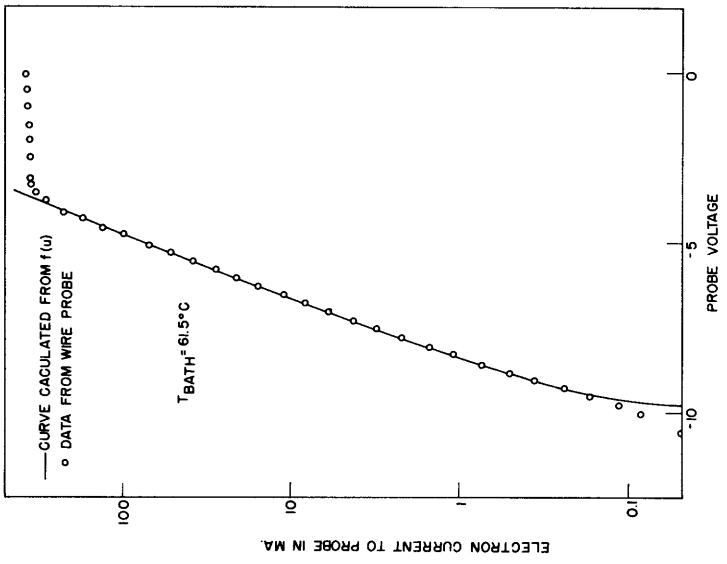

Fig. 12
Comparison of theoretical probe curve with experiment for 61.5°C bath.

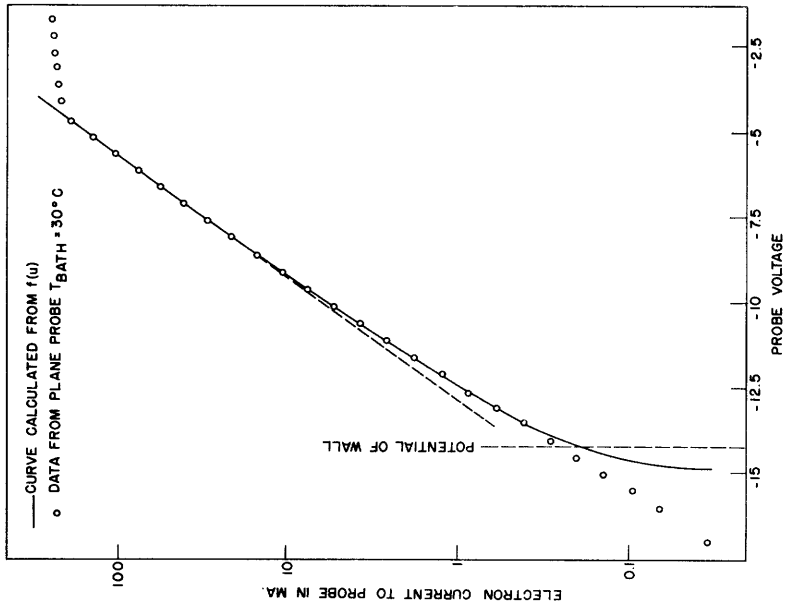

Fig. 11
Comparison of theoretical probe curve with experiment for 30°C bath.

Agreement between theory and experiment is not as good at a bath temperature at 22°C. This may be because mean-free paths are of the order of tube radius at this pressure; one would therefore expect the theory to break down.

Because inelastic collisions causing excitation and ionization are occurring in the same energy region as inelastic collisions with the wall, it seems difficult at the present time to determine the rate of electron transfer through velocity-space giving rise to the depleted distribution, and hence to calculate the electron-electron interaction cross section. When quantitative values for metastable concentrations as well as excitation and metastable ionization probabilities become available, then a reasonable calculation of electron-electron interaction cross section will be possible.

VIII. Radial Potential and Density Distributions

A. Ambipolar Diffusion Theory

Let us review briefly the ambipolar diffusion theory of Schottky (17). Both electrons and positive ions are diffusing out of the plasma to the tube walls. In the steady state this diffusion current $\bar{\Gamma}$ is the same for both positive ions and electrons, and hence we write

$$\bar{\Gamma} = -D_- \nabla n_- - \mu_- \bar{E} n_- \quad \text{for electrons} \tag{7}$$

and

$$\bar{\Gamma} = -D_+ \nabla n_+ + \mu_+ \bar{E} n_+ \quad \text{for positive ions} \tag{8}$$

where

$D_\pm$ = diffusion constant for electrons or positive ions

$n_\pm$ = density of electrons or positive ions

$\mu_\pm$ = mobility of electrons or positive ions

$\bar{E}$ = electric field (radial for a cylindrical discharge).

In the plasma of the arc n_- and n_+ are very nearly equal, so we assume

$$n_- = n_+ = n. \tag{9}$$

With this simplification we can eliminate $\bar{\Gamma}$ from Eqs. 7 and 8 and obtain

$$\bar{E} = \frac{D_- - D_+}{\mu_- + \mu_+} \left(- \frac{\nabla n}{n} \right). \tag{10}$$

Since $D_- >> D_+$ and $\mu_- >> \mu_+$, we have as a further approximation

$$\bar{E} \approx \frac{D_-}{\mu_-} \left(- \frac{\nabla n}{n} \right). \tag{11}$$

In cylindrical coordinates $\nabla n = dn/dr$ since n is a function of r only. Equation 11 thus becomes

$$-Edr = \frac{D_-}{\mu_-} \frac{dn}{n}$$

from which

$$V_p = -\int Edr = \frac{D_-}{\mu_-} \ln\left(\frac{n}{n_o}\right) \tag{12}$$

where we have set the plasma potential $V_p = 0$ at $n = n_o$. For a Maxwellian distribution $D_-/\mu_- = kT_-/e$ and Eq. 12 reduces to

$$n = n_o \exp\left(eV_p/kT_-\right) \tag{13}$$

which is the familiar Boltzmann density formula.

If we eliminate $\bar{E}$ from Eqs. 7 and 8 (again letting $n_- = n_+ = n$), we can solve for the diffusion current $\bar{\Gamma}$ and obtain

$$\bar{\Gamma} = -D_a \nabla n \tag{14}$$

where D_a is the ambipolar diffusion constant and is given by

$$D_a = \frac{D_-\mu_+ + D_+\mu_-}{\mu_+ + \mu_-}. \tag{15}$$

Ionization in the plasma of the arc discharge can take place in two ways: by direct or by cumulative ionization. When electrons ionize gas atoms by single collisions, it is known as direct ionization. When electrons raise gas atoms to an excited state as a result of a first collision and later ionize the excited atoms with a second collision, the process is known as cumulative ionization. Clearly the rate of ionization in the direct process will be proportional to the electron density n_-, while the rate of ionization in the cumulative, two-step process will be proportional to n_-^2. Each ionization results in the creation of a new free electron.

The rate of creation of new electrons in a unit volume must be equal to the rate at which they diffuse out, i.e. be equal to the divergence of the diffusion current $\bar{\Gamma}$. Thus for direct ionization

$$\nabla \cdot \bar{\Gamma} = \nu_i n_- \tag{16}$$

where ν_i is the average number of ionizing collisions made per second by one electron. The magnitude of ν_i will depend on: (a) the ionization probability as a function of electron energy and (b) the actual electron-energy distribution. Since probe measurements in this research and in Killian's work (3) have shown the energy distribution to be practically independent of distance from the tube axis, ν_i can be assumed to be independent of spacial coordinates. From Eq. 14 the above equation becomes

$$\nabla^2 n + \frac{\nu_i}{D_a} n = 0 \tag{17}$$

where $n_- = n$. For our case, we have cylindrical geometry. We impose the boundary condition that $n = 0$ at $r = R'$, where r is the radial distance from the tube axis and R' is the effective radius of the tube for diffusion theory, i.e. the radial distance at which n would go to zero were it not for the presence of a sheath at the tube wall.

Assuming that n is a function of r only, we find that for cylindrical coordinates and the above boundary condition the solution of Eq. 17 is given by a Bessel function of order zero. That is

$$n(r) = n_o J_o\left(\frac{2.405r}{R'}\right) \tag{18}$$

where n_o = plasma density at the axis ($r = 0$).

It can be shown that R' should exceed the actual tube radius R by $3/4\ \lambda$, where λ is the mean-free path of the electrons. However, this is true when the diffusion takes place for electrons of all energies, whereas only the high energy electrons in the plasma penetrate the sheath and reach the wall.

In the derivation of Eq. 17 it was assumed that the ionization was a direct, one-step process. In the case of cumulative ionization the rate of creation of free electrons will be proportional not to n_- but to n_-^2. This makes Eq. 17 nonlinear. Spenke (18) has recently solved this nonlinear equation, and the resulting function $\mathcal{N}(2.92r/R')$ is shown in Fig. 13 along with $J_o(2.4r/R')$ for comparison. As would be expected, the $\mathcal{N}$ curve resulting from cumulative ionization dips down more sharply from the tube axis than the J_o curve arising from direct ionization.

From Eq. 12 we see that for direct ionization the plasma potential is given by

$$V_p = \frac{D_-}{\mu_-} \ln\left[J_o\left(\frac{2.405r}{R'}\right)\right] \tag{19}$$

whereas for cumulative ionization

$$V_p = \frac{D_-}{\mu_-} \ln\left[\mathcal{N}\left(\frac{2.92r}{R'}\right)\right] \tag{20}$$

where $D_-/\mu_- = kT_-/e$ for a Maxwellian distribution.

B. Comparison of Diffusion Theory with Experiment

The various members of the telescope assembly serve as probe collectors positioned from tube axis to tube wall. The plasma potential or density, as obtained from each of these probes, represents the average taken over the length of the probe. Hence it would seem appropriate to plot radial potential or density data in the form of a step function, as shown in Fig. 14, where the width of each step represents the finite length of each probe. A smooth curve can be drawn through the steps, and it is reasonable to

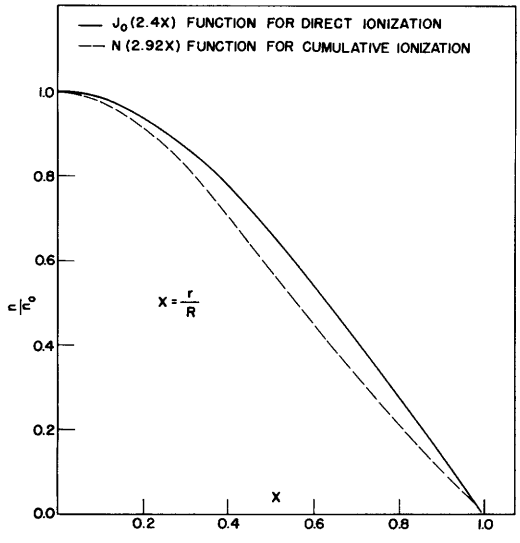

Fig. 13

Radial density distributions from diffusion theory.

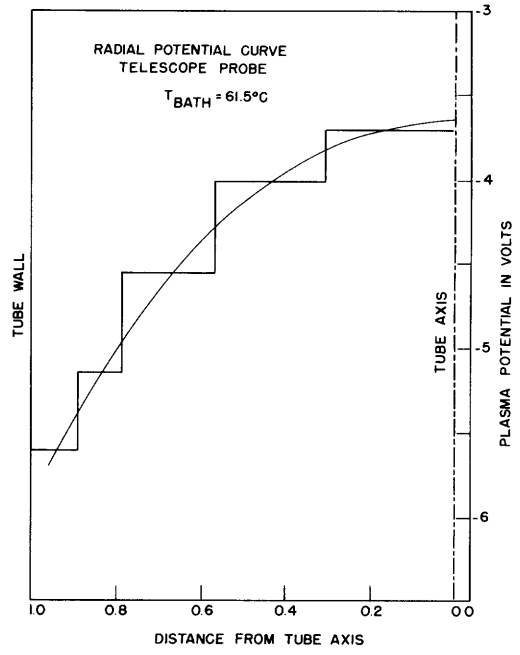

Fig. 14

Radial variation in plasma potential as a step function.

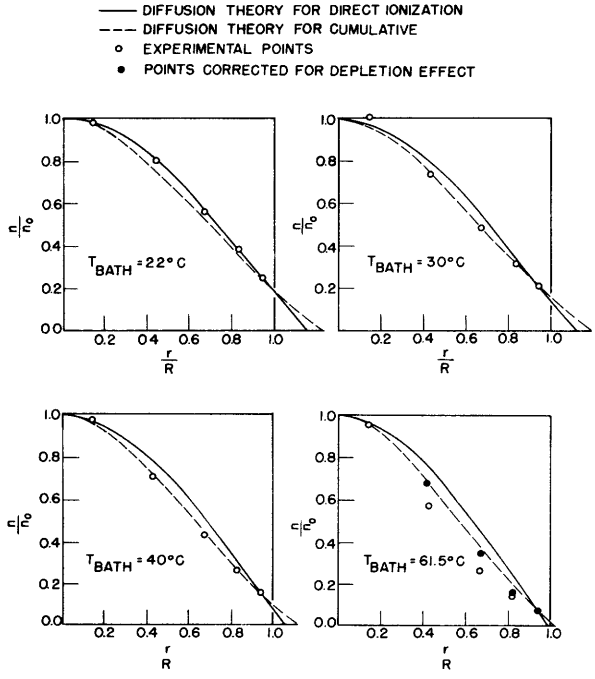

Fig. 15

Comparison of experimental radial density distributions with diffusion theory.

assume that this curve is a fair representation of the continuous plasma variation in potential from tube axis to tube wall. The smooth curve suggests, in turn, that we arbitrarily assign the mid-point of each probe segment as the representative point for the radial distance of that probe from the tube axis.

In this way the experimental points have been plotted in Fig. 15, where the observed radial density distribution is compared with the J_o and $\mathcal{N}$ curves for direct and cumulative ionization respectively. The value of R' has been selected in each case to make a good fit between theory and experiment near the wall. At 30°C and 40°C bath temperature the cumulative ionization theory seems to be a better fit. At 22°C the direct ionization theory is a little better. However, at this low pressure the mean-free path of the electrons is the order of the tube radius. Therefore, the applicability of diffusion theory is somewhat doubtful.

At 61.5°C bath temperature the observed density distribution dips below the cumulative ionization curve. This is believed to be the result of plasma-density depletion due to the larger area of those probes located away from the tube axis. This theory is borne out by comparing the probe currents obtained from the swivel probe and wire probe at the same bath temperatures. Both of these collectors are located at the tube axis, but the swivel probe has approximately four times the area of the wire probe (0.60 cm^2 compared with 0.13 cm^2). At 22°C, 30°C, and 40°C, the ratio of electron current at the swivel probe to electron current at the wire probe remains fixed, indicating that no depletion effect is taking place, whereas at 61.5°C the ratio is down by 30 percent. One can also observe a definite darkening of the plasma in the region surrounding the swivel probe when it is maintained at or above plasma potential. All of these facts indicate that at 61.5°C bath temperature (0.035 mm Hg), the finite area of the probe can cause an appreciable decrease in plasma density about the probe. If one makes a linear correction with the probe area of the experimental densities (based on the difference in densities as measured with plane and wire probes at the axis), points are obtained which lie more nearly on the cumulative ionization curve at 61.5°C.

We have already pointed out that R' - R should equal 3/4 λ when diffusion to the wall takes place for electrons of all energies. It was also observed that in our case only the high-energy electrons penetrate the sheath, and that therefore one would expect R' - R to be greater than 3/4 λ (in general, λ increases with the electron-energy increase). Nevertheless, we find that R' - R $\approx$ 3/4 λ when one calculates the mean-free path λ from Brode's curves (16) for electrons of energy kT_-. This is illustrated in the following table.

T_{bath}	Pressure	λ(for kT_-)	$\frac{3/4\,\lambda}{R}$	$\frac{R' - R}{R}$
22°C	0.00175 mm	2.3 cm	0.64	0.24
30°C	0.0034	1.0	0.28	0.20
40°C	0.0076	0.4	0.11	0.12
61.5°C	0.035	0.07	0.02	0.027

The actual mean-free paths of electrons are probably smaller than those obtained for collisions with mercury atoms due to electron-electron interactions. Thus the above agreement may be pure chance; that is, the mean-free path of the fast electrons which diffuse to the wall may be just enough smaller than the values taken from Brodé's curve to give approximate agreement with those same values calculated for an energy kT_-.

The theoretical plasma potential variations with radius are compared with experiment in Fig. 16. At 22°C the plasma potential has been calculated from

$$\frac{kT_-}{e} \ln \left[J_o\left(\frac{2.4r}{R'}\right)\right].$$

For the higher bath temperatures

$$\frac{kT_-}{e} \ln \left[\mathcal{M}\left(\frac{2.92r}{R'}\right)\right]$$

has been used. T_- was obtained from the upper slope of the plane- (swivel-) probe curve in each case. The agreement seems to be well within the experimental error, even though it is not quite correct to substitute kT_-/e for D_-/μ_- when the distribution

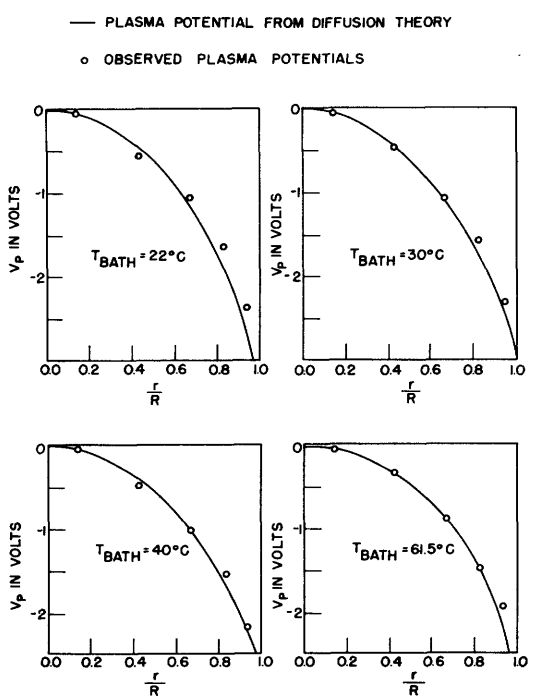

Fig. 16
Comparison of experimental radial potential distributions with diffusion theory.

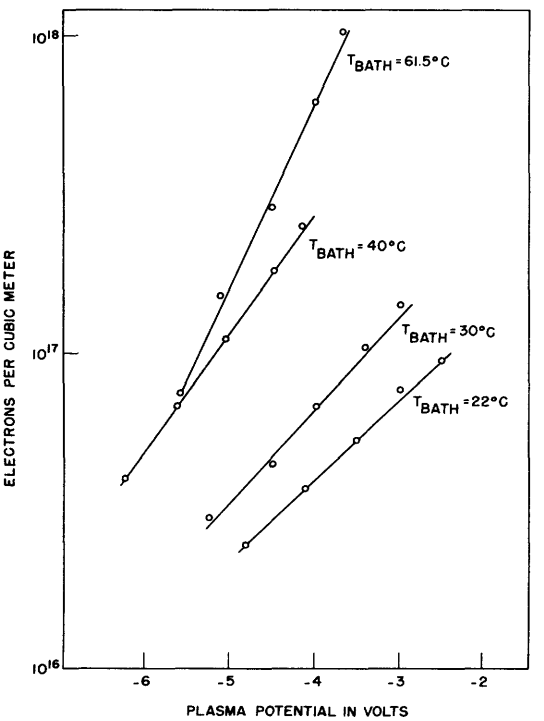

Fig. 17
Log density vs plasma potential from tube axis to wall.

is not perfectly Maxwellian. Indeed, to say that T_- as obtained from the upper slope of the plane-probe curve is an electron temperature loses its meaning in the face of a non-Maxwellian distribution.

A direct determination of D_-/μ_- can be obtained by plotting log n_- (obtained from Eq. 1 when $V = V_p$) vs plasma potential V_p for the telescope probes at each bath temperature. This has been done in Fig. 17. Reference to Eq. 12 shows that the resulting linear plots should have a slope of $0.434\ \mu_-/D_-$. When these slopes are converted to temperature units, the resulting temperatures are lower than those obtained from the upper slope of the probe curves themselves. At 20°C, 30°C, 40°C, and 61.5°C the temperatures are 18.5 percent, 10 percent, 7 percent, and 10 percent low, respectively. This is exactly what we should expect, since D_-/μ_- must be less than kT_-/e for a distribution depleted from a Maxwellian in the high-energy region, where kT_-/e represents the slope of the probe curve at low energies.

IX. Conclusions Regarding the Ionization Process in the Arc

In the previous section we saw that the radial potential and density distributions in the arc seemed to show better agreement with diffusion theory when cumulative ionization was assumed. From these facts alone, however, it is hardly safe to infer the type of ionizing process, since the difference between the theoretical radial density distributions for direct and cumulative ionization processes is not large. A more straightforward approach is to calculate the rate of direct ionization in the plasma from the known ionization probability and electron-energy distribution. If this calculated rate of ionization falls short of the observed rate (as obtained from the positive-ion current to the wall), the difference must be due to cumulative ionization. The theoretical distribution function given in Eq. 5 and illustrated in Figs. 11 and 12 has been used for this calculation at 22°C bath temperature, since it exhibits a reasonably good fit with experiment over the required energy range. The distribution must be displaced in velocity-space to take care of the drift effects (at 22°C this increases the direct ionization by a factor of two). The positive-ion wall current due to ionization calculated in this way is 2.10 amp/m^2 compared with the observed wall current of 4.58 amp/m^2. This would indicate that even at 22°C bath temperature (0.00175 mm Hg) a direct process accounts for only half of the ionization; the remainder is presumably cumulative.

For bath temperatures of 30°C and above, the density of high-energy electrons capable of direct ionization is even less than at 22°C, indicating that cumulative ionization predominates. These results are substantially in agreement with the work of Klarfeld (15), who concluded that for mercury-arc pressures above 0.001 mm Hg cumulative ionization is taking place.

Acknowledgment

The author is indebted to Professor W. B. Nottingham for his many valuable suggestions and constant interest in this research, and to Professor W. P. Allis for his considerable help with the theory.

References

1. I. Langmuir, H. Mott-Smith: Gen. Elec. Rev. 26, 731, 1923; 27, 449, 538, 616, 810, 1924; J. Frank. Inst. 196, 751, 1923
2. I. Langmuir, L. Tonks: Phys. Rev. 34, 876, 1929
3. T. Killian: Phys. Rev. 35, 1238, 1930
4. I. Langmuir, H. Mott-Smith: Gen. Elec. Rev. 27, 449, 1924
5. I. Langmuir, H. Mott-Smith: Gen. Elec. Rev. 27, 616, 1924; I. Langmuir, L. Tonks: Phys. Rev. 34, 876, 1929
6. M. L. E. Oliphant: Proc. Roy. Soc. 127, 373, 1930
7. C. Kentz: Phys. Rev. 44, 891, 1933
8. C. Kentz: Phys. Rev. 38, 377, 1931; 43, 181, 776, 1933
9. M. L. E. Oliphant: Proc. Roy. Soc. 132, 631, 1931
10. W. Molthan: Z. Physik 98, 3-4, 227, 1935
11. B. Klarfeld: J. Tech. Phys. (U.S.S.R.) 5, 913, 1938
12. M. J. Druyvesteyn: Z. Physik 64, 790, 1930
13. R. H. Sloane, E. I. R. MacGregor: Phil. Mag. 18, 193, 1934
14. W. B. Nottingham: Phys. Rev. 55, 203, 1939
15. B. Klarfeld: J. Tech. Phys. (U.S.S.R.) 5, 924, 1938
16. R. B. Brode: Phys. Rev. 35, 504, 1930
17. W. Schottky: Physik. Z. 25, 342, 635, 1924
18. E. Spenke: Z. Physik 127, 221, 1950

APPENDIX

SUMMARY OF DATA

T = 22°C	i_+ (ma)	i_- (ma)	T_- (°K)	V_{plasma} (volts)	Area (cm^2)	i_+ dens. (amp/m^2)	i_- dens. (amp/m^2)	electrons per $m^3_{-16} \times 10$
Plane Probe	0.505	157.	23,800	-3.7	0.60	8.42	2620	
Wall Probe	0.0423	13.0	23,500	-4.35	0.923	4.58	1410	
Wire Probe	0.157	48.5		-2.5	0.133	11.8	3650	9.52
Cyl No. 1	0.377	117.		-3.0	0.396	9.52	2950	7.70
Cyl No. 2	0.335	109.		-3.5	0.537	6.25	2070	5.40
Cyl No. 3	0.139	47.3		-4.1	0.331	4.20	1430	3.73
Cyl No. 4	0.112	42.1		-4.8	0.441	2.54	955	2.50
T = 30°C								
Plane Probe	0.624	210.	18,800	-4.25		10.4	3500	
Wall Probe	0.0444	13.9	18,600	-4.8		4.8	1510	
Wire Probe	0.219	64.		-3.0		16.5	4810	14.2
Cyl No. 1	0.448	141.		-3.4		11.3	3560	10.5
Cyl No. 2	0.365	125.		-4.0		6.80	2330	6.85
Cyl No. 3	0.152	51.		-4.5		4.60	1540	4.53
Cyl No. 4	0.121	46.		-5.25		2.75	1040	3.06
T = 40°C								
Plane Probe	0.897	317.	14,340	-5.6		15.0	5290	
Wall Probe	0.050	16.5	14,300	-6.1		5.42	1790	
Wire Probe	0.331	100.		-4.15		24.9	7520	25.3
Cyl No. 1	0.652	218.		-4.5		16.5	5500	18.5
Cyl No. 2	0.48	177.		-5.05		8.94	3300	11.1
Cyl No. 3	0.189	68.		-5.63		5.72	2060	6.92
Cyl No. 4	0.140	53.5		-6.25		3.18	1210	4.06
T = 61.5°C								
Plane Probe	2.28	820.	10,400	-4.85		38.0	13650	
Wall Probe	0.063	28.	10,200	-5.25		6.83	3030	
Wire Probe	1.00	352.	9,530	-3.70		75.2	26500	105.
Cyl No. 1	1.57	615.		-4.0		39.6	15500	62.5
Cyl No. 2	0.982	396.		-4.55		18.3	7380	29.3
Cyl No. 3	0.294	127.		-5.13		8.88	3840	15.2
Cyl No. 4	0.189	84.		-5.6		4.28	1900	12.0